

Study on tool wear and surface roughness in machining of particulate aluminum metal matrix composite-response surface methodology approach

M. Seeman · G. Ganesan · R. Karthikeyan ·
A. Velayudham

Received: 18 March 2008 / Accepted: 3 September 2009 / Published online: 22 September 2009
© Springer-Verlag London Limited 2009

Abstract Metal matrix composites (MMC) have become a leading material among composite materials, and in particular, particle reinforced aluminum MMCs have received considerable attention due to their excellent engineering properties. These materials are known as the difficult-to-machine materials because of the hardness and abrasive nature of reinforcement element-like silicon carbide particles (SiC_p). In this study, an attempt has been made to model the machinability evaluation through the response surface methodology in machining of homogenized 20% SiC_p LM25 Al MMC manufactured through stir cast route. The combined effects of four machining parameters including cutting speed (s), feed rate (f), depth of cut (d), and machining time (t) on the basis of two performance characteristics of flank wear (VB_{max}) and surface roughness (R_a) were investigated. The contour plots were generated to study the effect of process parameters as well as their interactions. The process parameters are optimized using desirability-based approach response surface methodology.

Keywords Metal matrix composites (MMC) · Response surface methodology (RSM) · Tool wear (VB_{max}) · Surface roughness (R_a) · Contour plots

1 Introduction

Metal matrix composites (MMC) are the new class of materials and are rapidly replacing conventional materials in various engineering applications such as the aerospace and automobile industries. Some of the typical applications are bearings, automobile pistons, cylinder liners, piston rings, connecting rods, sliding electrical contacts, turbo charger impellers, space structures, etc. [1]. The most popular reinforcements are silicon carbide (SiC) and alumina (Al_2O_3). Aluminum, titanium, and magnesium alloys are commonly used as the matrix phase. The density of most of the MMCs is approximately one third that of steel, resulting in high-specific strength and stiffness [2]. It is possible to produce high-quality MMC components to near-net shape through various manufacturing techniques, but additional machining is unavoidable to achieve the desired surface quality and dimensional tolerance for efficient assembly [3].

Several studies have been done in order to examine the efficiency of different cutting tool materials, such as cemented carbide, coated carbide, and diamond in turning, milling, drilling, reaming, and threading of MMC materials. The main problem while machining MMC is the extensive tool wear caused by the very hard and abrasive reinforcements. Manna et al. [4] investigated the machinability of Al/SiC MMC and found that no built-up edge (BUE) is formed during machining of Al/SiC MMC at high speed and low depth of cut and also observed a better surface finish at high speed with low feed rate and low depth of cut.

M. Seeman (✉) · G. Ganesan
Department of Manufacturing Engineering, Annamalai University,
Annamalainager 608002, Tamilnadu, India
e-mail: seeman_au575@rediffmail.com

R. Karthikeyan
Department of Mechanical Engineering,
Birla Institute of Science and Technology (BITS),
Dubai, United Arab Emirates

A. Velayudham
Combat Vehicles Research and Development Establishment
(CVRD), Ministry of Defense,
Avadi, Chennai 600054, Tamilnadu, India

Ibrahim Ciffchi et al. [5] studied the effects of SiC volume fraction and its size together during turning of SiC reinforced 2014Al alloy MMC and found that coated cutting tools performed better than uncoated cutting tools in terms of tool wear and uncoated cutting tools produced better surface finish particularly at lower cutting speeds. Tamer Ozben et al. [6] investigated the mechanical properties and the effects of machining parameters on tool wear and surface roughness of silicon carbide particulate (SiCp) reinforced aluminum MMC for different volume fraction. It was observed that the increase in reinforcement addition produced better mechanical properties such as impact toughness and hardness. The machinability properties of the selected material were studied and higher SiCp reinforcement produced a higher tool wear. The surface roughness was generally affected by feed rate and cutting speed. Davim et al. [7] made a correlation between the chip compression ratio and shear plane angle or chip deformation during MMCs turning. The results showed shear angle decreased with the chip compression ratio. On the contrary, the chip deformation increased with chip compression ratio. The merchant model gives, in general, an overestimation of the shear plane angle value in cutting of aluminum matrix composites.

Kannan et al. [8] studied tool wear, surface integrity, and chip formation during machining of Al-MMC under both wet and dry condition. The turning results showed that the tool life was increased at higher cutting speeds in influence of coolant but the surface quality was deteriorated. This was mainly due to the flushing away of the partially debonded particulates from the machined surface, thus, forming higher percentage of pit holes and voids. Suresh Kumar Reddy et al. [9] studied quality of components produced during end milling of Al/SiC particulate metal–matrix composites (PMMCs). The results showed that the presence of the reinforcement enhances the machinability in terms of both surface roughness and lower tendency to clog the cutting tool, when compared to a non-reinforced Al alloy. These results would serve to understand that the end milling machining process can provide better inputs to ensure better machining of Al/SiC PMMC and are expected to lead technological and economical gains with the use of Al/SiC PMMC in various industrial applications by replacing Al alloys.

Kevin Chou and Jie Liu [10] studied the machining of Al/SiC composite material using chemical vapor deposited (CVD) diamond tools and investigated the cutting force, temperature, and tool wear. Finite element simulation of cutting temperature and micrograph study were also conducted to evaluate processes parameter effects and to get an insight of tool wear mechanisms. The results indicated that the tool wear was sensitive to cutting speed and feed rate, and the dominant wear mechanism was the

coating failure due to high stress. Ibrahim Ciftci et al. [11] studied the influence of different particle size of SiC and cutting speed on tool wear and surface roughness during machining of Al/SiC MMC using cubic boron nitride (CBN) cutting tool. The results showed that tool wear was mainly observed on flank side with a strong influence by abrasive reinforcement. It was also found that CBN cutting tool was unsuitable for machining MMC containing with SiC particle size of 110 μm due to the heavy fracture of the cutting edge and nose.

Paulo Davim [12] compared the performance of brazed polycrystalline diamond (PCD) with CVD diamond coated tools during machining of MMCs. The results indicated that PCD insert tools have longer tool life and better surface roughness and also found CVD diamond coated tools show short life, as tool wear evolution becomes very fast after coating rupture [13]. Pramanik et al. [14] developed a mechanics model for predicting the forces when machining aluminum alloy based MMCs reinforced with ceramic particles. The predictions revealed that the force due to chip formation is much higher than those due to plowing and particle fracture.

El Gallab et al. [15] studied PCD tool performance during high-speed turning of 20% Al/SiC MMC and found that PCD tools suffered excessive edge chipping and crater wear during the machining of the MMC. Palanikumar [16] developed a model for surface roughness through response surface method (RSM) while machining GFRP composites. Four factors five level central composite rotatable design matrix was employed to carry out the experimental investigation. Analysis of variance (ANOVA) was used to check the validity of the model. Jenn-Tsong Horng et al. [17] made an attempt to model the machinability evaluation through the RSM while machining Hadfield steel. Results indicated that the flank wear was influenced principally by the cutting speed and the interaction effect of feed rate with nose radius of tool, the cutting speed and the tool corner radius had statistic significance on the surface roughness.

Muthukrishnan et al. [18] developed two modeling techniques used to predict the surface roughness namely ANOVA and ANN. In ANOVA, it is revealed that the feed rate has highest physical as well as statistical influence on the surface roughness (51%) right after the depth of cut (30%) and the cutting speed (12%). ANN methodology consumes lesser time giving higher accuracy. Hence, optimization using ANN is the most effective method compared with ANOVA. Oktem et al. [19] developed an effective methodology to determine the optimum cutting conditions leading to minimum surface roughness while milling of mold surfaces by coupling RSM with a developed genetic algorithm (GA). Results showed that RSM model was further interfaced with the GA; the GA reduced the surface roughness value in the mold cavity

from 0.412 to 0.375 μm corresponding to about 10% improvement. Choudhury et al. [20] developed the first- and second-order tool-life models at 95% confidence level for turning high strength steel. The tool-life models are developed in terms of cutting speed, feed rate, and depth of cut using response surface methodology and design of experiment. Authors found that the tool-life contours were useful in determining the optimum cutting conditions for a given tool life.

From the literature it is found that the machining of Al-MMC is an important area of research, but only very few studies have been carried out on optimization of flank wear (VB_{max}) and surface roughness (Ra) while machining of particulate aluminum metal matrix composite (PAMMC). Hence, the main objective of the present work is to optimize tool wear and surface roughness while machining LM25 AlSiCp metal matrix composite using RSM.

2 Design of experiment based on response surface methodology

In order to investigate the influence of machining parameters on the flank wear (VB_{max}) and surface roughness (Ra) four principal machining parameters such as the cutting speed (s), feed rate (f), depth of cut (d), and machining time (t) were taken. In this study, these machining parameters were chosen as the independent input variables. The desired responses were the flank wear (VB_{max}) and the surface roughness (Ra) which are assumed to be affected by the above four principal machining parameters.

The response surface methodology was employed for modeling and analyzing the machining parameters in the turning process so as to obtain the machinability performances of VB_{max} and Ra. In the RSM, the quantitative form of relationship between the desired response and independent input variables is represented as follows:

$$Y = F(s, f, d, t) \quad (1)$$

Where Y is the desired response, and F is the response function (or response surface). In the procedure of analysis, the approximation of Y was proposed using the fitted second-order polynomial regression model, which is called the quadratic model. The quadratic model of Y can be written as follows:

$$Y = a_0 + \sum_{i=1}^4 a_i X_i + \sum_{i=1}^4 a_{ii} X_i^2 + \sum_{i < j}^4 a_{ij} X_i X_j \quad (2)$$

Where a_0 is constant, a_i , a_{ii} , and a_{ij} represent the coefficients of linear, quadratic, and cross product terms, respectively. X_i reveals the coded variables that correspond

to the studied machining parameters. The coded variables X_i , $i=1,2,3,4$ are obtained from the following transformation equations:

$$X_1 = \frac{s-s_0}{\Delta s} \quad (3)$$

$$X_2 = \frac{f-f_0}{\Delta f} \quad (4)$$

$$X_3 = \frac{d-d_0}{\Delta d} \quad (5)$$

$$X_4 = \frac{t-t_0}{\Delta t} \quad (6)$$

Where X_1 , X_2 , X_3 and X_4 are the coded values of parameters s , f , d and t respectively; s_0 , f_0 , d_0 and t_0 are the values of s , f , d and t , respectively at zero level. Δs , Δf , Δd and Δt are the intervals of variation in s , f , d and t , respectively. The flank wear (VB_{max}) and surface roughness (Ra) indicated as $Y_{VB_{\text{max}}}$ and Y_{Ra} , respectively, were analyzed as responses. The purpose of using this quadratic model Y in this study was not only to investigate over the entire factor space but also to locate the region where the response approaches its optimum or near optimal value of the desired target.

The necessary data for building the response models are generally collected by the experimental design. In this study, the collections of experimental data were adopted using central composite design (CCD). The factorial portion of CCD is a full factorial design with all combinations of the factors at two levels (high, +1 and low, -1) and composed of the eight star points and seven central points (coded level 0) which is the midpoint between the high and low levels. The star points are at the face of the cubic portion on the design which corresponds to a α value of 1 and this type of design is commonly called the face-centered CCD. Table 1 shows the levels of four machining parameters and their ranges. The parameter levels were chosen based on the early work [21] and by the correlated processing parameters of mechanical equipment. The experimental plans were carried out using the stipulated conditions based on the face-centered CCD involving 31 runs in the coded form as shown in Table 2. The design was generated and analyzed using MINITAB statistical package.

3 Experimental work

The main goal of the experiment was to establish a relationship between the machining parameter and the machinability performance, which included flank wear

Table 1 Cutting parameter and their levels

Control Parameters	Unit	Symbol	Levels		
			-1	0	+1
Cutting speed	m/min	<i>s</i>	50	100	150
Feed rate	mm/rev	<i>f</i>	0.05	0.15	0.30
Depth of cut	mm	<i>d</i>	0.5	1.0	1.5
Machining time	min	<i>t</i>	2	4	6

(VB_{\max}) and surface roughness (Ra). The LM 25 aluminum alloy (7 Si, 0.33 Mg, 0.3 Mn, 0.5 Fe, 0.1 Cu, 0.1 Ni, 0.2 Ti) reinforced with green-bonded silicon carbide particles of size 25 μm with 20% volume fraction manufactured through stir-casting route was used for experimentation. The turning tests were performed on PSG 141 lathe with the following specifications: Height of center 177.5 mm,

swing in gap 520 mm, spindle speed range 30–1,600 rpm, feed range 0.05–3.5 mm/rev, and main motor power 2.25 kW.

The ISO specification of the tool used for the turning operation was WIDAX tool holder PT GNR 2525 M16. The insert used was uncoated carbide tool insert (K10) with the following specifications: TNMG 160404 IC 428. The

Table 2 Design matrix with responses (flank wear (VB_{\max}) and surface roughness (Ra))

Run	Coded factors				Actual factors				Response variable	
	X_1	X_2	X_3	X_4	<i>s</i>	<i>f</i>	<i>d</i>	<i>t</i>	Y_1 (VB_{\max} , mm)	Y_2 (Ra, μm)
1	-1	0	0	0	50	0.15	1.0	4	0.29	3.03
2	1	0	0	0	150	0.15	1.0	4	0.52	1.41
3	0	-1	0	0	100	0.05	1.0	4	0.30	2.85
4	0	1	0	0	100	0.30	1.0	4	0.55	1.59
5	0	0	-1	0	100	0.15	0.5	4	0.31	2.91
6	0	0	1	0	100	0.15	1.5	4	0.56	1.56
7	0	0	0	-1	100	0.15	1.0	2	0.30	1.94
8	0	0	0	1	100	0.15	1.0	6	0.71	2.02
9	-1	1	1	1	50	0.30	1.5	6	0.47	2.33
10	1	-1	-1	-1	150	0.05	0.5	2	0.49	1.39
11	-1	-1	1	1	50	0.05	1.5	6	0.45	2.54
12	1	1	-1	-1	150	0.30	0.5	2	0.65	1.92
13	-1	-1	-1	1	50	0.05	0.5	6	0.48	1.76
14	1	1	1	-1	150	0.30	1.5	2	0.70	2.03
15	-1	-1	-1	-1	50	0.05	0.5	2	0.22	2.42
16	1	1	1	1	150	0.30	1.5	6	0.28	2.98
17	-1	1	-1	1	50	0.30	0.5	6	0.43	2.25
18	1	-1	1	-1	150	0.05	1.5	2	0.63	1.92
19	-1	1	-1	-1	50	0.30	0.5	2	0.42	2.24
20	1	-1	1	1	150	0.05	1.5	6	0.35	2.01
21	-1	1	1	-1	50	0.30	1.5	2	0.38	2.14
22	1	-1	-1	1	150	0.05	0.5	6	0.36	2.03
23	-1	-1	1	-1	50	0.05	1.5	2	0.47	1.63
24	1	1	-1	1	150	0.30	0.5	6	0.29	1.82
25	0	0	0	0	100	0.15	1.0	4	0.42	2.25
26	0	0	0	0	100	0.15	1.0	4	0.41	2.24
27	0	0	0	0	100	0.15	1.0	4	0.43	2.23
28	0	0	0	0	100	0.15	1.0	4	0.44	2.25
29	0	0	0	0	100	0.15	1.0	4	0.40	2.24
30	0	0	0	0	100	0.15	1.0	4	0.41	2.32
31	0	0	0	0	100	0.15	1.0	4	0.42	2.24

size of the work piece was 90 mm diameter and 250 mm length. The machining operations were carried out as per the conditions given by the design matrix at random to avoid systematic errors.

In the present study, the tool wear area was considered as the criterion that would affect the results of cutting process. The measurement of the width of the flank wear land of the cutting tool was used to evaluate the tool wear as shown in Figs. 1 and 2. The maximum value of flank wear (VB_{max}) was adopted as the machinability evaluation of machining MMC. Here, the flank wear was measured with CLEMAX optical microscope. The average surface roughness (R_a), which is mostly used in industries, was taken for this study. The surface roughness was measured by using MITU-TOYO SURF III surface tester. The specifications of the tester was as follows: speed of traverse 2–5 mm/s, range of traverse 2.5 mm, driving power 2 VA and measuring range 0.3–100 μm .

4 Mathematical modeling

4.1 Development of mathematical model

The mathematical relationship between responses (i.e., VB_{max} , R_a) and machining parameters was established using the experimental test results shown in Table 2 was obtained from planned set of experiments based on CCD. The coefficients of regression analysis for flank wear (VB_{max}) and surface roughness (R_a) is shown in Tables 3 and 4 along with their P value of the parameters, higher order, and interactions.

The P value of regression analysis of VB_{max} in Table 3 indicates that linear, square, and interactions of cutting speed with feed rate are most significant, whereas linear, square, and interactions of depth of cut and machining time are not so significant. Similarly, the P value of regression analysis of R_a in Table 4 indicates that linear, square, and interaction of cutting speed and feed rate are the most significant, whereas linear, square, and interactions of depth

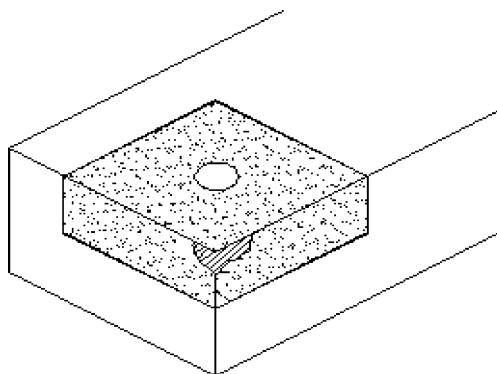
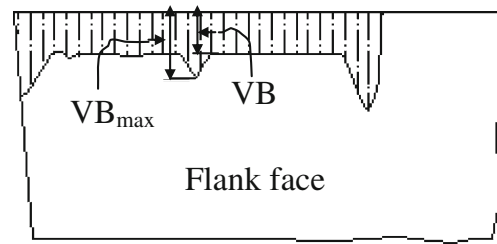


Fig. 1 Flank wear on a cutting tool insert



VB_{max} – Maximum flank wear
 VB – Flank wear

Fig. 2 Measurement of flank wear

Table 3 Regression analysis of flank wear (VB_{max})

Symbol	Coefficient	P value
Constant	0.20316	<0.006
X_1 (s, m/min)	0.00568	<0.000
X_2 (f, mm/rev)	-1.54010	<0.001
X_3 (d, mm)	-0.13469	0.271
X_4 (t, min)	-0.02926	0.336
X_1^2	0.00002	<0.001
X_2^2	3.39259	<0.002
X_3^2	0.08267	0.159
X_4^2	0.00517	0.159
$X_1 X_2$	0.00692	<0.000
$X_1 X_3$	-0.00003	0.913
$X_1 X_4$	0.00009	0.116
$X_2 X_3$	-0.01018	0.911
$X_2 X_4$	-0.03462	0.144
$X_3 X_4$	0.00438	0.449

Table 4 Regression analysis of surface roughness (R_a)

Symbol	Coefficient	P value
Constant	1.3544	<0.000
X_1 (s, m/min)	0.0056	<0.034
X_2 (f, mm/rev)	9.7498	<0.000
X_3 (d, mm)	-0.2458	0.322
X_4 (t, min)	-0.0236	0.700
X_1^2	-0.0000	<0.001
X_2^2	-12.6981	<0.000
X_3^2	0.1812	0.132
X_4^2	0.0088	0.234
$X_1 X_2$	-0.0203	<0.000
$X_1 X_3$	-0.0005	0.317
$X_1 X_4$	0.0000	0.873
$X_2 X_3$	-0.0646	0.730
$X_2 X_4$	-0.0447	0.345
$X_3 X_4$	-0.0056	0.632

Table 5 Summary of regression analysis

Responses	<i>S</i> value	R^2 (%)	Adjusted R^2 (%)
Flank wear (VB_{\max})	0.0225622	98.22	96.66
Surface roughness (Ra)	0.0460248	99.37	98.83

of cut and machining time are not so significant as the P values are more than 0.05. The machining time includes both cutting speed and feed rate; the influence of machining time could not be seen distinctly from the P value. But its influence is very much reflected by the significant contribution of cutting speed and feed rate. Actually, machining time is the ratio between the length of cut and the product of spindle speed and feed rate. Equations 7 and 8 represent the regression model equation for flank wear (VB_{\max}) and surface roughness (Ra).

Regression equation for flank wear (VB_{\max}):

$$\begin{aligned}
 Y_{VB_{\max}} = & 0.20316 + 0.00568X_1 - 1.54010X_2 \\
 & - 0.13469X_3 - 0.02926X_4 - 0.00002X_1^2 \\
 & + 3.39259X_2^2 + 0.08267X_3^2 + 0.00517X_4^2 \\
 & + 0.00692X_1X_2 - 0.00003X_1X_3 \\
 & + 0.00009X_1X_4 - 0.01018X_2X_3 \\
 & - 0.03462X_2X_4 + 0.00438X_3X_4 \quad (7)
 \end{aligned}$$

Regression equation for surface roughness (Ra):

$$\begin{aligned}
 Y_{Ra} = & 1.3544 + 0.0056X_1 + 9.7498X_2 - 0.2458X_3 \\
 & - 0.0236X_4 - 12.6981X_2^2 + 0.1812X_3^2 \\
 & + 0.0088X_4^2 - 0.0203X_1X_2 - 0.0005X_1X_3 \\
 & - 0.0646X_2X_3 - 0.0447X_2X_4 - 0.0056X_3X_4 \quad (8)
 \end{aligned}$$

Where $Y_{VB_{\max}}$, Y_{Ra} are responses of flank wear (VB_{\max}) and surface roughness (Ra) and X_1 , X_2 , X_3 , and X_4 represent the decoded values of cutting speed (s), feed rate (f), depth

of cut (d), and machining time (t), respectively. Single variable terms have the main effect on the response and interaction, square effect also considered. The developed mathematical model can be used to analyze the effects of machining parameters on VB_{\max} and Ra in machining of particulate metal matrix composite.

Where S is the estimated standard deviation about the regression line, R^2 also called the coefficient of determination which is calculated as $R^2 = (SS \text{ Regression}) / (SS \text{ Total})$, where SS stands for sums of squares. R^2 (Adj) is an approximately unbiased estimate of the population R^2 . The S value being measurement of error it is smaller the better. So, the mathematical model for VB_{\max} is less deviated from the regression line than that of Ra (Table 5).

The higher value of R^2 is better to determine the coefficients of regression equation. So the coefficient in the regression equation for Ra has been determined more effectively than that of VB_{\max} . The closeness of the adjusted R^2 with R^2 determines the fitness of model [16]. In both causes, the adjusted R^2 value is closer to the R^2 value.

4.2 Analysis of the developed mathematical models

The ANOVA and F ratio test have been performed to justify the goodness of fit of the developed mathematical models. The calculated values of F ratios for lack-of-fit have been compared to standard values of F ratios corresponding to their degrees of freedom to find the adequacy of the developed mathematical models. The F ratio calculated from ratio of Mean Sum of Square of source to Mean Sum of experimental error.

The ANOVA tables shown in Tables 6 and 7 for flank wear (VB_{\max}) and surface roughness (Ra). The standard percentage point of F distribution for 95% confidence limit is 4.06. As shown in Tables 6 and 7, the F value is 3.90 and 3.07 for lack-of-fit is smaller than the standard value of 95% confidence limit. Thus, both the models are adequate in 95% confidence limit. It is also seen that from the P values, both VB_{\max} and Ra models linear, square, and interaction effects of cutting speed and feed rate are significant.

Table 6 Analysis of variance for flank wear (VB_{\max})

Source	Degree of freedom	Sum of square	Adjusted mean square	F value	P value
Regression	14	0.449313	0.032081	63.02	0.000
Linear	4	0.395555	0.004609	9.05	0.001
Square	4	0.020544	0.005136	10.09	0.000
Interaction	6	0.033033	0.005505	10.82	0.000
Residual error	16	0.008145	0.000509		
Lack of fit	10	0.007059	0.000706	3.90	0.055
Pure error	6	0.001086	0.000181		
Total	30	0.457277			

Table 7 Analysis of variance for surface roughness (Ra)

Source	Degree of freedom	Sum of square	Adjusted mean square	F value	P value
Regression	14	5.38488	0.384634	181.58	0.000
Linear	4	4.75576	0.131625	62.14	0.000
Square	4	0.36508	0.091270	43.09	0.000
Interaction	6	0.26404	0.044006	20.77	0.000
Residual error	16	0.03389	0.002118		
Lack of fit	10	0.02835	0.002835	3.07	0.091
Pure error	6	0.00554	0.000924		
Total	30	5.41877			

5 Results and discussion

5.1 Effect of machining parameters on flank wear (VB_{max})

During turning operation of multiphase materials like MMC, the cutting wedge experienced abrasion as well as force fluctuation due to grinding of harder abrasive particles and material heterogeneity respectively. Based on the mathematical model given by Eq. 7 developed through experimental observations and response surface methodology, studies have been made to analyze the effect of the various process parameters on the flank wear (VB_{max}). The contour plots were drawn for various combinations. The number represent in the plot is flank wear (VB_{max}).

In Fig. 3, it is clear that the flank wear (VB_{max}) increases with the increase in the cutting speed (s). At lower cutting speed, tool wear is lesser extent, which can be attributed to formation of larger size unstable BUE due to high contact pressure and friction. The formation of unstable larger BUE at low cutting speed is shown in Fig. 4, which protects the cutting wedge from further wear [22]. But with increase in cutting speed, an increase in tool wear is observed which could be due to generation of higher temperature at higher

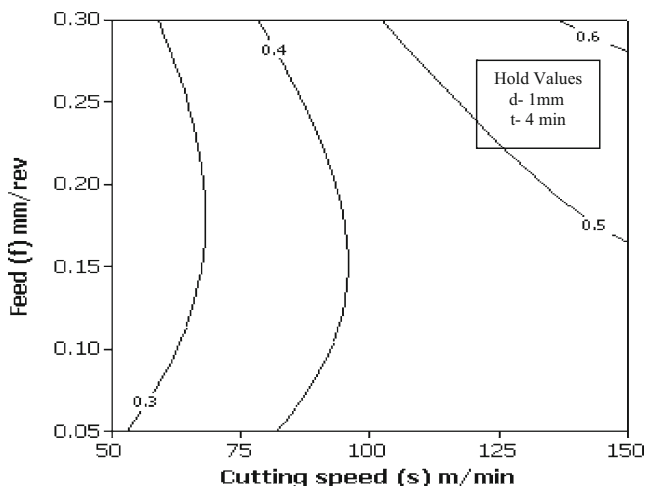


Fig. 3 Effect of cutting speed (s) and feed rate (f) on flank wear (VB_{max})

cutting speed and associated thermal softening and deterioration of form stability of the cutting wedge [23]; also, the flank wear increases with increase in feed rate. It is due to BUE formed on flank face that changes the geometry of the tool [24]. Higher flank wear was observed at the range of 0.25–0.30 mm/rev of feed rate (f) and 125–150 m/min of cutting speed (s). Figure 5 clearly indicates that the reduction in the size of BUE due to increase in cutting speed and associated thermal influence.

Figures 6 and 7 indicate the flank wear (VB_{max}) at low and high cutting speed (s); flank wear (VB_{max}) area increases with increase of cutting speed. In order to examine the tool wear mechanism in detail, the worn cutting tools were micrographed using the SEM. Sodium hydroxide (NaOH, 1 M) solution was used to remove the work material adhered onto the surface of the tools. From Fig. 6a and b, distinct abrasive wear grooves could be seen on the flank face while turning Al/SiC_p metal matrix composite material at low cutting speed (50 m/min) caused by abrasive nature of the hard SiC particle present in the workpiece materials. The grooves that formed on the tool face were filled with the workpiece material. The adhering layer somewhat protected the tools flank face against further abrasion [25]. When the cutting speed increased to

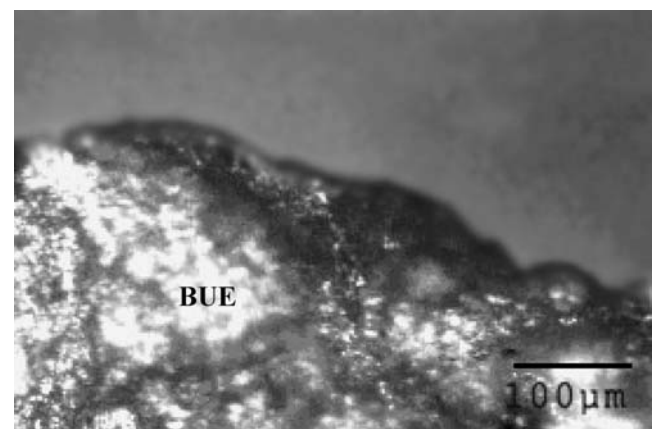


Fig. 4 Optical image of BUE formation at $s=50$ m/min, $f=0.05$ mm/rev, $d=0.5$ mm, and $t=2$ min

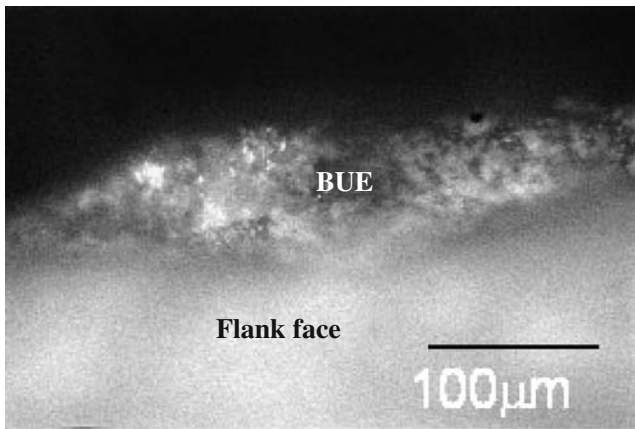
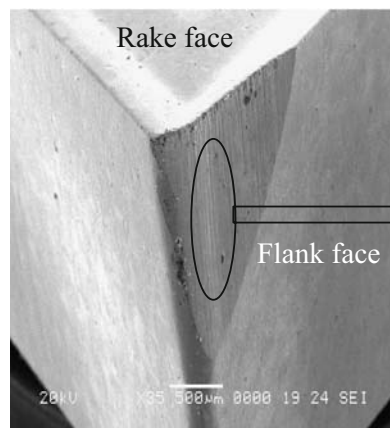


Fig. 5 Optical image of BUE formation at $s=150$ m/min, $f=0.05$ mm/rev, $d=0.5$ mm, and $t=2$ min

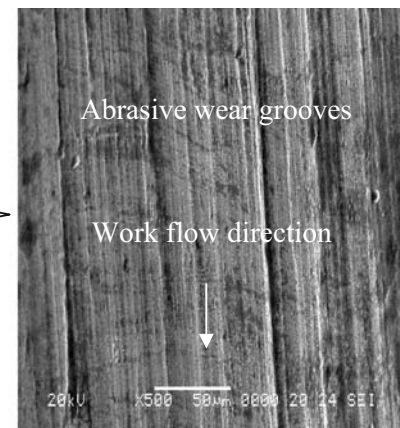
150 m/min, abrasive and adherence of work material on to the flank face is seen which is mainly due to generation of high contact pressure and temperature between work and tool; chip–tool interfaces during machining of MMC is given in Fig. 7a, b. Surface topographies of the tool indicate that the main wear mechanism of cemented carbide tool is abrasive and adhesive wear [15].

Figure 8 shows the influence of machining time (t) and depth of cut (d) on flank wear (VB_{max}). The effect of time on wear has three stages: initial, steady-state, and worn-out regions. The effect of time will be more pronounced in the third stage. In the present study, the maximum time period considered is 9 min. The wear regime might not have reached the third stage with in the period. Hence, the effect of time is found to be less significant. The depth of cut (d) also has least influence factor on flank wear (VB_{max}) in machining of MMC [26]. If the depth of cut is beyond 1 mm, the flank wear (VB_{max}) increases due to increase in area of contact, normal load, and friction. This, in turn, increases temperature, which will cause

Fig. 6 Scanning electron micrographs of K10 tool $s=50$ m/min, $f=0.15$ mm/rev, $d=1$ mm, and $t=4$ min



(a) Flank wear



(b) Higher magnification of flank face

work softening and thus results in increased flank wear (VB_{max}).

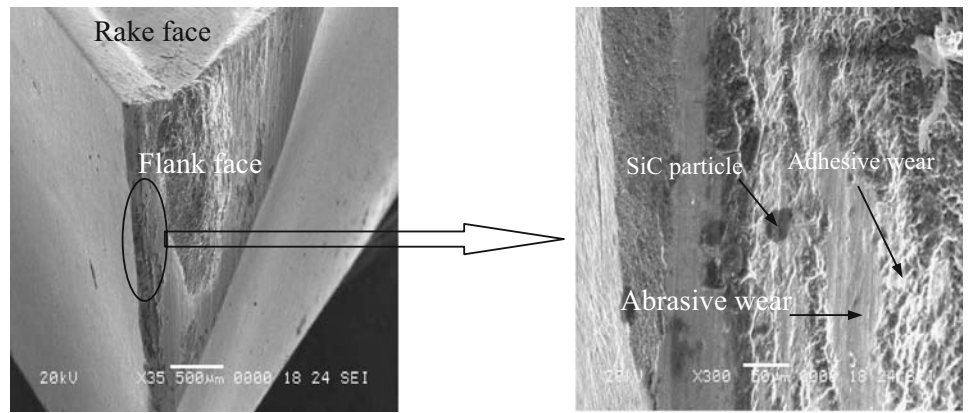
5.2 Effect of machining parameters on surface roughness (R_a)

Based on the mathematical model given by Eq. 8, the study of the effects of various machining parameters on surface roughness (R_a) has been made so as to analyze the suitable parametric combinations that can be made for achieving controlled surface roughness. The contour plots were drawn for various combinations. The number represent in the plot is surface roughness (R_a).

From Fig. 9, the increase in feed rate (f) increases the surface roughness (R_a). With the lower feed rates, the BUE forms readily and is accompanied by feed marks resulting in increased roughness. With the increase in feed rate beyond 0.2 mm/rev, the rate of increase in surface roughness (R_a) is less due to the reduced effect of BUE [20]; also, the surface roughness (R_a) decreases as the cutting speed (s) increases. At low cutting speed (s), the unstable larger BUE is formed and also the chips fracture readily producing the rough surface. As the cutting speed (s) increases, the BUE vanishes, chip fracture decreases, and, hence, the roughness decreases [21]. The best surface finish was achieved at the lowest feed rate and highest cutting speed combination.

The effect of depth of cut (d) and machining time (t) on the surface roughness (R_a) is shown in Fig. 10. The depth of cut low as 0.5–1 mm less surface roughness observed. But increase in depth of cut (d) beyond 1 mm, results in high normal pressure and seizure on the rake face and promotes the BUE formation. Hence, the surface roughness (R_a) increases along with increase in depth of cut (d). The surface roughness (R_a) increases with the increase in the machining time (t) due to increase in wear and subsequent vibration [27]. This result is observed commonly in all metal cutting processes.

Fig. 7 Scanning electron micrographs of K10 tool $s=150$ m/min, $f=0.15$ mm/rev, $d=0.5$ mm, and $t=4$ min



(a) Flank wear

(b) Higher magnification of flank face

6 Analysis for optimization of the responses

One useful approach to optimization of multiple responses is to use the simultaneous optimization technique popularized by Derringer and Suich [28]. Their procedure introduces the concept of desirability functions. The general approach is to first convert each response Y into an individual desirability function d_i that varies over the range.

$$0 \leq d_i \leq 1 \tag{9}$$

Where if the response Y is at its goal or target, then $d_i=1$, and if the response is outside an acceptable region, $d_i=0$. The weight of the desirability function for each response defines its shape. For each response, one can select a weight (r_i) to emphasize or de-emphasize the target. Finally, the individual desirability functions are combined to provide a measure of the composite or overall desirability of the multiresponse system [29]. This measure of

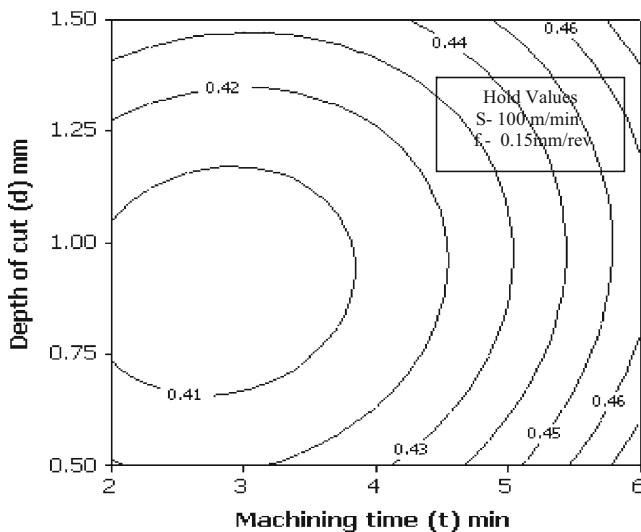


Fig. 8 Effect of depth of cut (d) and machining time (t) on flank wear (VB_{max})

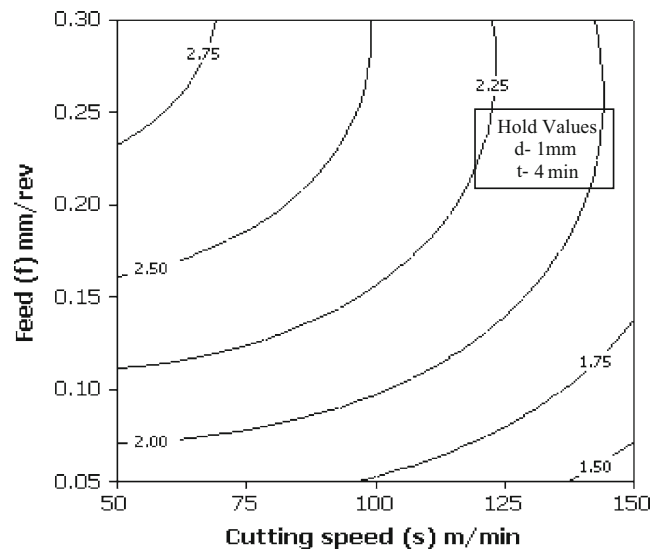


Fig. 9 Effect of cutting speed (s) and feed rate (f) on surface roughness (R_a)

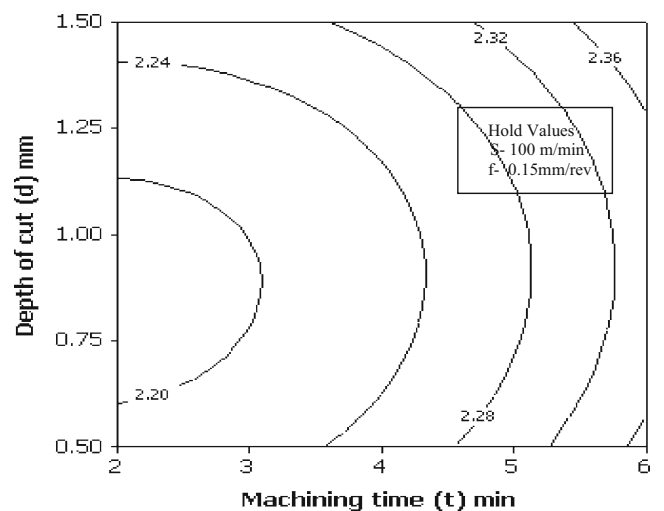


Fig. 10 Effect of machining time (t) and depth of cut (d) on surface roughness (R_a)

Fig. 11 Optimum results for minimum flank wear (VB_{max})

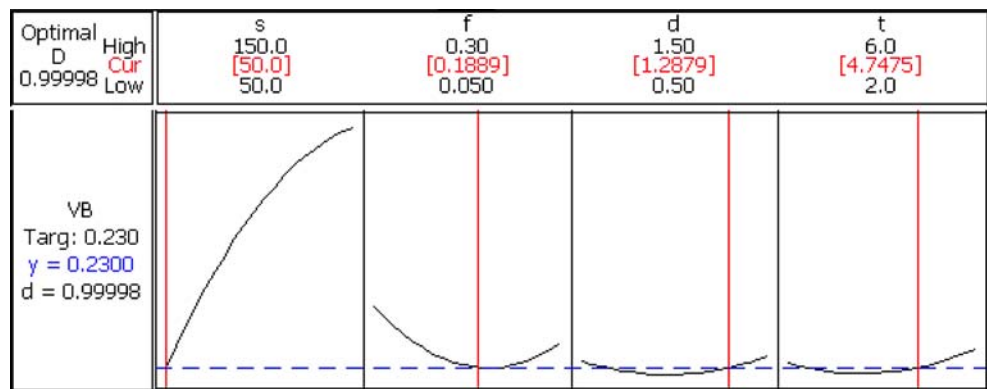


Fig. 12 Optimum results for minimum surface roughness (Ra)

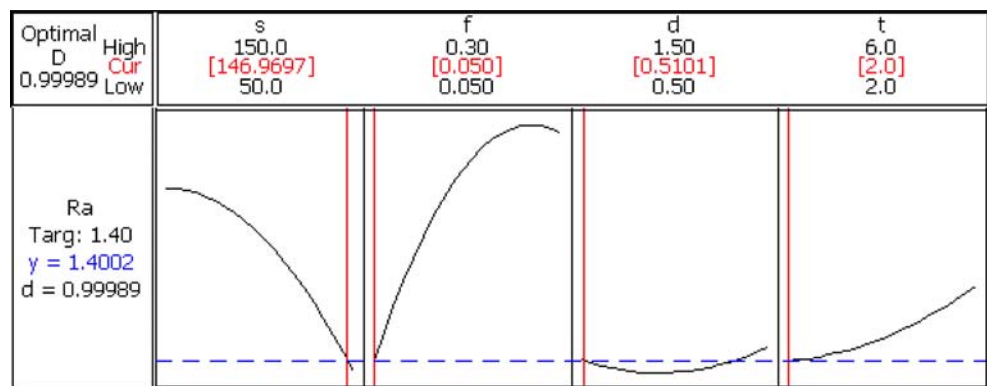
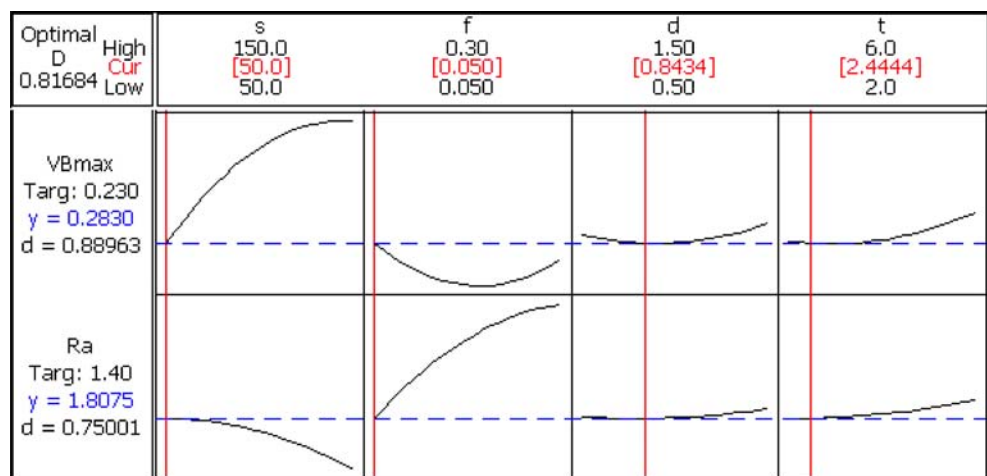


Fig. 13 Optimum results for minimum flank wear (VB_{max}) and surface roughness (Ra)



composite desirability is the weighted geometric mean of the individual desirability for the responses. The optimal operating conditions can then be determined by maximizing the composite desirability. In the present investigation, the response parameters are chosen to maximize the overall desirability as follows:

$$D = (d_1^{i_1} d_2^{i_2})^{1/(i_1+i_2)} \quad (10)$$

Where d_1 and d_2 are the desirability functions for flank wear (VB_{\max}) and surface roughness (Ra), respectively, and i_1 and i_2 are the importance of transformed response parameters of d_1 and d_2 . Usually, a reduced gradient algorithm with multiple starting points is employed that maximizes the composite desirability to determine the optimal input variable settings. Most of the standard statistical software packages (Minitab, Design expert, etc.) employ this popular technique for response optimization. In the present case, Minitab was used to optimize the response parameters.

The optimization plot for flank wear has been shown in Fig. 11. The goal was to minimize the flank wear. The upper value and target has been fixed at 0.71 and 0.23 mm, respectively. The parameter setting for achieving a flank wear as low as of 0.23 mm are cutting speed (s) 50 m/min, feed rate (f) 0.18 mm/rev, depth of cut (d) 1.28 mm, and machining time (t) 4.75 min. The desirability of optimization has been calculated as 0.99998, i.e., all parameters are within their working range.

The optimization plot for surface roughness has been shown in Fig. 12. The goal was to minimize the surface roughness. The upper value and target has been fixed at 3.03 and 1.40 μm , respectively. The parameter setting for achieving a surface roughness as low as of 1.4002 μm has been predicted as cutting speed (s) 146.96 m/min, feed rate (f) 0.05 mm/rev, depth of cut (d) 0.5 mm, and machining time (t) 2 min. The desirability of optimization has been calculated as 0.99989, i.e., all the parameters are within their working range.

Optimization plot for both the responses is shown Fig. 13. The objective is to minimize both responses considered at a time. As the composite desirability is close to 1, it can be concluded that the parameters are within their working range. The optimized values of cutting parameters are cutting speed (s) 50 m/min, feed rate (f) 0.05 mm/rev, depth of cut (d) 0.84 mm, and machining time (t) 2.4 min.

7 Conclusions

The experimental analysis highlights that the machining criteria like VB_{\max} , Ra in composite machining are greatly influenced by the various predominant machining param-

eters considered in the present study. Response surface methodology used in the present research work has proved its adequacy to be an effective tool for analysis of the composite machining process. From the investigation, the following conclusions are drawn.

1. Cutting speed and feed rate of the regression models are found to be more significant when compared to other parameters. The proposed models for flank wear and surface roughness are found to be adequate and can be used to predict the characteristics within the experimental range.
2. Formation of BUE significantly affects the tool wear at low speeds whereas thermal softening plays important role at higher speeds and feed rates. Surface topographies of the tool indicate that the main wear mechanism of cemented carbide tool is abrasive and adhesive wear.
3. The surface roughness is significantly affected by BUE formation at low speeds. The surface roughness is low at higher speed and lower feed rate ranges. Depth of cut increases the increase in surface roughness.
4. The optimal machining parametric combination is obtained using desirability function. Cutting conditions such as cutting speed 50 m/min, feed rate 0.05 mm/rev, depth of cut 0.84 mm, and machining time 2.4 min can be used to achieve the minimum flank wear of 0.283 mm and minimum surface roughness of 1.8075 μm .

References

1. Ding X, Liew WYH, Liu XD (2005) Evaluation of machining performance of MMC with PCBN and PCD tools. *Wear* 259:1225–1234
2. Quan Y, Ye B (2003) The effect of machining on the surface properties of SiC/Al composites. *J Mater Process Technol* 138:464–467
3. Hung NP, Loh NL, Xu ZM (1996) Cumulative tool wear in machining metal matrix composites part II: machinability. *J Mater Process Technol* 58:114–120
4. Manaa A, Bhattacharya B (2003) A study on machinability of Al/SiC-MMC. *J Mater Process Technol* 140:711–716
5. Ciftci I, Turker M, Seker U (2004) Evaluation of tool wear when machining SiCp-reinforced Al-2014 alloy matrix composites. *Mater Des* 25:251–255 Technical report
6. Ozben T, Kilickap E, Cakir O (2008) Investigation of mechanical and machinability properties of SiC particle reinforced Al-MMC. *J Mater Process Technol* 198:220–225
7. Davim JP, Silva J, Baptista AM (2007) Experimental cutting model of metal matrix composites (MMCs). *J Mater Process Technol* 183:358–362
8. Kannan S, Kishawy HA (2008) Tribological aspects of machining aluminum metal matrix composites. *J Mater Process Technol* 198:399–406
9. Suresh Kumar Reddy N, Shin K-S, Minyang Y (2008) Experimental study of surface integrity during end milling of Al/SiC particulate metal-matrix composites. *J Mater Process Technol* 201:574–579

10. Kevin Chou YR, Liu J (2005) CVD diamond tool performance in metal matrix composite machining. *Surf Coat Technol* 200:1872–1878
11. Ciftci I, Turker M, Seker U (2004) CBN cutting tool wear during machining of particulate reinforced MMCs. *Wear* 257:1041–1046
12. Paulo Davim J (2007) Application of merchant theory in machining particulate metal matrix composites. *Mater Des* 28:2684–2687
13. Paulo Davim J (2002) Diamond tool performance in machining metal–matrix composites. *J Mater Process Technol* 128:100–105
14. Pramanik A, Zhang LC, Arsecularatne JA (2006) Prediction of cutting forces in machining of metal matrix composites. *Int J Mach Tools Manuf* 46:1795–1803
15. El-Gallab M, Sklad M (1998) Machining of Al/SiC particulate metal-matrix composites part I & II. *J Mater Process Technol* 83 (151–158):277–285
16. Palanikumar K (2007) Modeling and analysis for surface roughness in machining glass fibre reinforced plastics using response surface methodology. *Mater Des* 28:2611–2618
17. Horng J-T, Liu N-M, Chiang K-T (2008) Investigating the machinability evaluation of Hadfield steel in the hard turning with Al₂O₃/TiC mixed ceramic tool based on the response surface methodology. *J Mater Process Technol* 208(1–3):532–541
18. Muthukrishnan N, Paulo Davim J (2009) Optimization of machining parameters of Al/SiC-MMC with ANOVA and ANN analysis. *J Mater Process Technol* 209:225–232
19. Oktema H, Erzurumlu T, Kurtaran H (2005) Application of response surface methodology in the optimization of cutting conditions for surface roughness. *J Mater Process Technol* 170:11–16
20. Choudhury IA, El-Baradie MA (1998) Tool-life prediction model by design of experiments for turning high strength steel (290 BHN). *J Mater Process Technol* 77:319–326
21. Palanikumar K, Karthikeyan R (2007) Assessment of factors influencing surface roughness on the machining of Al/SiC particulate composites. *Mater Des* 28:1584–1591
22. Masounave J, Litwin J, Hamelin D (1994) Prediction of tool life in turning aluminum matrix composites. *Mater Des* 15:287–293
23. Kilickap E, Aksoy M, Inan A (2005) Study of tool wear and surface roughness in machining of homogenized SiC-p reinforced aluminum metal matrix composite. *J Mater Process Technol* 164–165:862–867
24. Hung NP, Boey FYC, Khor KA, Phua YS, Lee HF (1996) Machinability of aluminum alloys reinforced with silicon carbide particulates. *J Mater Process Technol* 56:966–977
25. Sahin Y (2005) The effects of various multi layer ceramic coatings on the wear of carbide cutting tools when machining metal matrix composites. *Surf Coat Technol* 199:112–117
26. Quigley Q, Monaghan J, O'Reilly P (1994) Factors affecting the machinability of an Al/SiC metal-matrix composite. *J Mater Process Technol* 43:21–36
27. Kannan S, Kishawy HA (2006) Surface characteristics of machined aluminum metal matrix composites. *Int J Mach Tool Manufac* 46:2017–2025
28. Derringer G, Suich R (1980) Simultaneous optimization of several response variables. *J Qual Technol* 12:214–219
29. Sarkar S, Sekh M, Mitra S, Bhattacharyya B (2008) Modeling and optimization of wire electrical discharge machining of γ -TiAl in trim cutting operation. *J Mater Process Technol* 205:376–387